Available online at www.sciencedirect.com
SCIENCE DIRECT®
Journal of Chromatography A, 1066 (2005) 55–70
JOURNAL OF CHROMATOGRAPHY A
www.elsevier.com/locate/chroma

Chromatographic evaluation of poly (*trans*-1,2-cyclohexanediyl-bis acrylamide) as a chiral stationary phase for HPLC

Qiqing Zhong[a], Xinxin Han[a], Lingfeng He[b], Thomas E. Beesley[b], Walter S. Trahanovsky[a], Daniel W. Armstrong[a,*]

[a] *Department of Chemistry, Iowa State University, Ames, IA 50011, USA*
[b] *Advanced Separation Technologies Inc, 37 Leslie Court, P.O. Box 297, Whippany, NJ 07981, USA*

Received 9 November 2004; accepted 15 December 2004
Available online 2 February 2005

Abstract

Chiral stationary phases (CSPs) based on polymeric (*R*,*R*)- or (*S*,*S*)-1,2-diaminocyclohexane (DACH) derivatives are synthesized. When bonded to 5 μm porous spherical silica gel, the poly (*trans*-1,2-cyclohexanediyl-bis acrylamide) based poly-cyclic amine polymer (P-CAP) stationary phases is proved to be effective chiral stationary phases that could be used in the normal-phase mode, polar organic mode and with halogenated solvents mobile phases, if desired. Since these are entirely synthetic CSPs, the elution order of all enantiomers can be reversed between the (*R*,*R*) P-CAP and (*S*,*S*) P-CAP columns. Because of the high loading of chiral selectors, the columns exhibit very high sample capacities. Thus, P-CAP columns are useful for preparative and semi-preparative enantiomeric separations. The application of these CSPs and optimization of their separations are discussed.

Keywords: P-CAP; Synthetic polymeric chiral stationary phases; Poly (*trans*-1,2-cyclohexanediyl-bis acrylamide); Preparative chiral separation

1. Introduction

Enantiomeric separations were thought to be difficult or impossible prior to the early 1980s with only a few enantiomeric resolutions reported [1–4]. By the late 1990s, advances in the field of analytical chiral separations have made the separation of enantiomers practical and even routine [1,5]. Over 100 chiral stationary phases (CSPs) were commercialized through the 1980s and 1990s [6–8]. Based on their structure, chiral selectors can be classified as macrocyclic, polymeric, π–π association, ligand exchange, miscellaneous and hybrid CSPs [6]. Generally, polymeric CSPs, with the exception of proteins, have a high loading of chiral selector on the surface of silica gel, thus they have the potential of high sample loading capacity. This feature makes them suitable for preparative purposes.

In 1926, Wieland et al. reported the synthesis of *trans*-1,2-diaminocyclohexane (DACH) for the first time [9]. This diamine has C_2 symmetry and its enantiomers can be resolved by recrystallization with D- or L-tartaric acid to give enantiomerically pure (1*R*,2*R*)- or (1*S*,2*S*)-DACH [10,11]. In industry, *trans*-1,2-diaminocyclohexane can be obtained as a byproduct from purification of 1,6-diaminohexane, which is a starting material for the manufacture of Nylon 66. Thus, enantiomerically pure DACH is commercially available at relatively low prices. Both the pure enantiomers and derivatives of *trans*-DACH can serve as powerful stereogenic ligands in asymmetric synthesis [12–16] or as components of chiral stationary phases in chiral chromatographic separations [17–26].

Polymeric CSPs have been used extensively for enantiomeric HPLC separations. Two types of chiral polymers

* Corresponding author. Tel.: +1 515 294 1394; fax: +1 515 294 0838.
E-mail address: sec4dwa@iastate.edu (D.W. Armstrong).

0021-9673/$ – see front matter © 2004 Elsevier B.V. All rights reserved.
doi:10.1016/j.chroma.2004.12.088

are used as CSPs. They can be classified by their origin. One group consists of naturally occurring polymers (such as proteins and linear carbohydrates) and their derivatives; the other is composed of purely synthetic polymers [27–29]. Unlike small molecule chiral selectors, which are usually bonded on to the surface of silica gel, chiral polymers can be bonded or coated on the surface of a silica gel support. Moreover, chiral polymers can also be crosslinked as a monolithic gel. The ability of chiral recognition by small molecular CSPs depends mainly on the structure of the small molecules. However, the mechanism of enantiomeric separation by polymeric CSPs is more complicated than that by small molecule CSPs because of the secondary structure of the polymers which may be critical for chiral recognition [7]. Generally, it is easier to increase the loading of polymeric chiral selectors onto the surface of a silica gel support than it is for small molecule-based covalently bonded CSPs. Therefore, synthetic or semi-synthetic polymeric CSPs may have a greater potential for high sample loading capacity.

The poly (*trans*-1,2-cyclohexanediyl-bis acrylamide) based stationary phases has been commercialized by Advanced Separation Technologies Inc. (Astec, Whippany, NJ, USA) with the commercial name of poly-cyclic amine polymer (P-CAP). P-CAP can be prepared from either (1*R*,2*R*)-DACH or (1*S*,2*S*)-DACH and thus (*R*,*R*) P-CAP or (*S*,*S*) P-CAP, respectively. These two chiral selectors are enantiomers. Thus, unlike most naturally occurring polymeric CSPs such as derivatized linear or branched carbohydrates and proteins, it is easy to obtain opposite selectivity using these synthetic polymeric chiral selectors.

2. Experimental

2.1. Materials

Porous spherical silica gel (diameter: 5 μm; pore size: 200 Å; pore volume: 0.9 ml/g; specific surface area: 213 m^2/g) was from Akzo Nobel, EKA Chemicals AB, Sweden. Acryloyl chloride and 1-methoxy-2-methyl-1-trimethylsyliloxy-1-propene were from Lancaster Synthesis, Inc, Pelham, NH. 3-Aminopropyltrimehoxysilane was from SILAR Lab, Scotia, NY. Anhydrous toluene, methylene chloride and chloroform were from Sigma-Aldrich. 4,4′-Azo-bis-4-cyanovaleric acid was from Fluka. Phosphorus pentachloride (*R*,*R*)- and (*S*,*S*)-diaminocyclohexane, and diisopropylethylamine were from Alfa Aesar, Ward Hill, MA. Absolute ethanol was obtained from AAPER Alcohol and Chemical Co., Shelbyville, KY, USA. Acetonitrile, 2-propanol, *n*-heptane, and methylene chloride were HPLC grade from Fischer, Fairlawn, NJ. Triethylamine, trifluoroacetic acid and acetic acid were ACS certified grade from Fisher Scientific. Water was deionized and filtered through activated charcoal and a 5 μm filter. Most analytes used in this study were from Sigma-Aldrich.

2.2. Synthetic procedure

The (*R*,*R*) P-CAP and (*S*,*S*) P-CAP columns were prepared as previously reported [30]. The stationary phases consisted of the chiral selector were covalently bonded to 5 μm porous spherical silica gel. The dimensions of the columns are 250 mm × 4.6 mm. The synthetic procedure is summarized below.

2.2.1. Preparation of (1R,2R)-cyclohexanediyl-bis acrylamide (DACH-ACR)

(1*R*,2*R*)-Diaminocyclohexane (12.1 g, 105.96 mmol) and diisopropylethylamine (36.3 ml, 210.18 mmol) were dissolved in 160 ml mixed anhydrous solvent (chloroform:toluene = 3:1 (v/v)). Acryloyl chloride (17.3 ml, 210.18 mmol) was added dropwise into the solution at 0 °C under nitrogen protection with stirring. The reaction was warmed up to room temperature for 2 h. The product was collected by filtration, washed with toluene and hexane, and dried at reduced pressure (0.1 mbar, 25 °C) over night to obtain 19.08 g white solid (yield: 81.6%).

TLC: Merck Kieselgel 60-F254; Eluent: CH_2Cl_2/MeOH 90/10, R_f = 0.56. Elemental analysis found: C 61.78%; H 8.41%; N 12.81%. Calculated for $C_{12}H_{18}N_2O_2$: C 64.83%; H 8.16%; N 12.61%. ^{1}H NMR (400 MHz, methanol-*d*4): δ 8.00 (s, 2H), 6.17–6.15 (m, 4H), 5.60 (dd, *J* =6.8 Hz, 5.2 Hz, 2H), 3.80–3.70 (m, 2H), 2.00–1.95 (m, 2H), 1.80–1.70 (m, 2H), 1.40–1.30 (m, 4H). ^{13}C NMR (methanol-*d*4): δ 166.7, 130.8, 125.3, 52.8, 31.9, 24.5.

2.2.2. Preparation of dichloride of 4,4′-azo-bis-4-cyanovaleric acid

To a suspension of phosphorous pentachloride (115.1 g, 552.48 mmol) in 576 ml of anhydrous methylene chloride is added a suspension of 4,4′-azo-bis-4-cyanovaleric acid (28.8 g, 138.24 mol) in 900 ml of anhydrous methylene chloride at −5 °C under nitrogen protection with continuous stirring. After 1 h, the reaction mixture was warmed up to room temperature and kept over night, and then filtered. The precipitate was dried under reduced pressure (0.1 mbar, 25 °C) to obtain 24.8 g of the title compound (yield: 73.7%).

2.2.3. Preparation of 3-aminopropyl silica gel (3-APSG-200)

To anhydrous slurry of 5 μm silica gel (85.7 g) dispersed in 850 ml of anhydrous toluene is added 3-aminopropyltrimethoxysilane (42 ml, 180.6 mmol) at room temperature. The mixture was heated to reflux for 5 h and filtered afterwards. The silica gel was dried at 105 °C over night to obtain 91.97 g 3-APSG-200 (weight gain: 7.4%). Elemental analysis found: C 3.22%, H 0.88%, N 0.88%.

2.2.4. Functionalization of 3-aminopropyl silica gel with the dichloride of 4,4′-azo-bis-cyanovaleric acid

To anhydrous slurry of 3-APSG-200 (88.5 g) dispersed in 742 ml anhydrous toluene is added a solution

of 1-methoxy-2-methyl-1-(trimethylsyliloxy)-1-propene (MMTP) (14.8 ml, 72.52 mmol) at −5 °C, followed by adding the solution of dichloride of 4,4′-azo-bis-4-cyanovaleric acid (9.98 g, 36.24 mmol) in 297 ml anhydrous toluene under nitrogen protection with mechanical stirring. The mixture was warmed up to room temperature (25 °C) for 5 h. The modified silica gel was filtered, and dried at reduced pressure (0.1 mbar, 25 °C) to obtain 95.9 g functionalized silica gel (3-APSG-AZO-200). The percentage of weight gain was 8.4%. Elemental analysis found: C 7.00%, H 1.10%, N 2.26%.

2.2.5. Preparation of (R,R) P-CAP

To a solution of (1*R*,2*R*)-DACH-ACR (14.0 g) in 1380 ml anhydrous, degassed chloroform, is added 3-APSG-AZO-200 (82.4 g) under nitrogen protection. The mixture was heated at 61 °C for 5 h and then heated to reflux for 1 h. After cooling down to room temperature, the reaction mixture was filtered, washed with methanol and acetone, and dried under vacuum (0.1 mbar, 60 °C) for 4 h to obtain 91.5 g (*R*,*R*) P-CAP bonded silica gel (weight gain: 11.1%). Elemental analysis found: C 12.83%, H 1.98%, N 2.69%.

2.3. Equipment

Chromatographic separations were carried out using an HP 1050 HPLC system with a UV VWD detector, an auto sampler, and computer-controlled HP ChemStation for LC data processing software. The mobile phases were degassed by purging compressed pure helium gas for 10 min. UV detection was carried out at 210, 254 or 264 nm for most of the probe compounds. All separations were carried out at room temperature (∼23 °C).

2.4. Column evaluation

The performance of (*R*,*R*) P-CAP and (*S*,*S*) P-CAP was evaluated in the normal-phase mode using *n*-heptane/ethanol, *n*-heptane/2-propanol and methylene chloride/methanol mobile phases; in polar organic phase mode using acetonitrile/methanol mobile phase.

2.5. Calculations

The chiral separation ability of CSPs can be quantitatively evaluated by retention factors (k'), selectivity factor (α), and resolution factor (R_s). Those parameters are defined as follows:

$$k'_1 = \frac{(t_1 - t_0)}{t_0} \quad (1)$$

$$k'_2 = \frac{(t_2 - t_0)}{t_0} \quad (2)$$

$$\alpha = \frac{t_2 - t_0}{t_1 - t_0} = \frac{k'_2}{k'_1} \quad (3)$$

$$R_s = \frac{2(t_2 - t_1)}{W_1 + W_2} \quad (4)$$

in which, t_1 and t_2 are the retention times of enantiomers; t_0 is the dead time and was estimated by using the peak resulting from the change in refractive index from the injection solvent on columns; W_1 and W_2 are the peak widths. To evaluate the efficiency of separation, the number of theoretical plates (N) is also used

$$N = 16\left(\frac{t_R}{W}\right)^2 \quad (5)$$

where t_R is the retention time of the peak and W is the peak width.

3. Results and discussion

3.1. The structure of P-CAP chiral selectors

Gasparrini and co-workers [19,20,31] used *trans*-1,2-cyclohexanediamine acrylamide as monomer to synthesize poly-DACH-ACR, which forms a crosslinked structure. In synthesizing the related P-CAP chiral stationary phase, the free radical initiator was immobilized on the surface of silica gel before the free radical polymerization process was carried out [30,32]. Therefore, P-CAP is basically a linear brush-type polymer with the DACH-ACR units as the branches. The idealized structure of (*R*,*R*) P-CAP CSP is shown in Fig. 1. The structure of (*S*,*S*) P-CAP CSP has the opposite configuration of each stereogenic center of the cyclohexyl units on (*R*,*R*) P-CAP.

3.2. Column performance

A total of 62 chiral compounds were separated on the P-CAP CSPs in the normal-phase mode (using two different solvent systems: traditional normal phase and a halogenated solvent mobile phase) and the polar organic mode combined. The majority of compounds were separated in the traditional normal-phase mode (heptane/ethanol). Table 1 shows the chromatographic data for 43 racemic compounds separated in the traditional normal-phase mode. Of these compounds, 23 were not separated in the polar organic mode. Sixteen out of 43 compounds were baseline separated.

Table 2 lists the enantioseparation data obtained for the polar organic mobile phase mode (34 compounds). The polar-organic mode is somewhat analogue to the normal-phase mode. The difference of mobile phase composition is the normal phase contains *n*-heptane while the polar-organic phase does not. Instead, the polar-organic phase has acetonitrile as its main solvent. There are 16 compounds separated in the polar organic mode only, but not in the normal phase modes. Twelve baseline separations were achieved in polar organic phase mode.

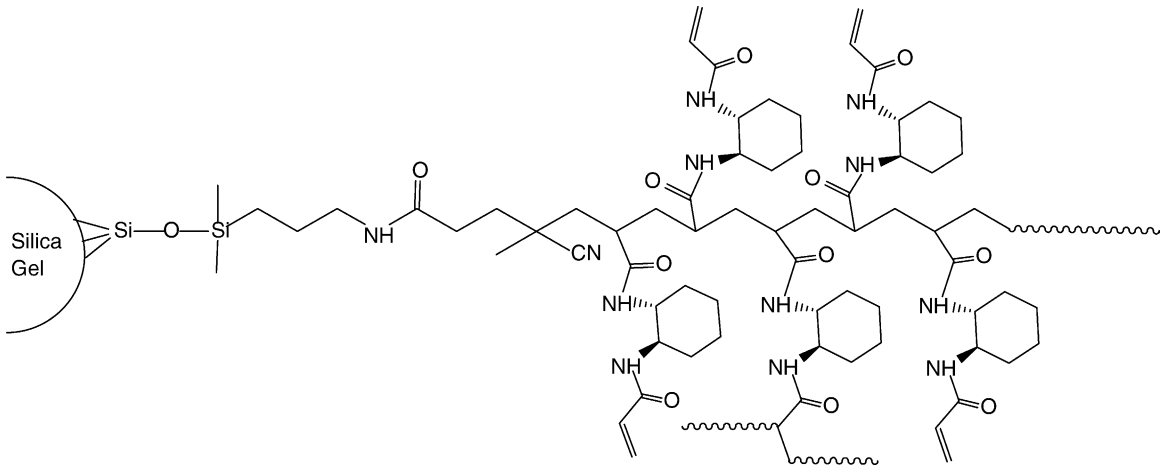

Fig. 1. The structure of (*R*,*R*) P-CAP chiral stationary phase.

Table 3 shows the enantioseparation data in the normal-phase mode with a halogenated solvent (methylene chloride) and other mobile phases (10 compounds). Methanol was used as a modifier for these separations. All 10 compounds separated using a methylene chloride-based mobile phase can also be separated in either the normal-phase mode (eight compounds) or polar organic mode (five compounds). Three compounds were enantioseparated in all three solvent systems (i.e. the traditional normal-phase mode, polar organic mode, and the normal-phase mode with halogenated solvent). One baseline enantiomeric resolution of 1,1′-bi-2-naphthol was achieved using a neat acetone mobile phase.

Because of the covalent linkage between the polymeric chiral selector and their solid support (5 μm porous silica gel), no degradation in column performance was observed even after more than 1000 injections in each mobile phase mode.

3.2.1. Retention behavior

Typical normal-phase retention (k') behavior of two analytes (A) 1,1′-bi-2-naphthol and (B) fipronil is shown in Fig. 2. The diagrams show that the first and second eluted enantiomers of each analyte plotted as a function of mobile phase composition with different ratios of ethanol and *n*-heptane. In both cases, the retention and selectivity are greatest when using ethanol/heptane 10/90 (v/v) as the mobile phase.

No data were available at 100% *n*-heptane because the elution times are extremely long. As can be seen, retention decreases with increasing the concentration of ethanol. Retention of all analytes tends to be minimal at ethanol concentration of ≥50% (by volume). However, it is interesting that even at 100% ethanol, the P-CAP column still gives an enantioselectivity (α) of 1.23 and resolution (R_s) of 1.15 for 1,1′-bi-2-naphthol.

Fig. 3 contains plots for the retention factor k'_1 of the first eluted enantiomer, selectivity factor α, and resolution R_s of

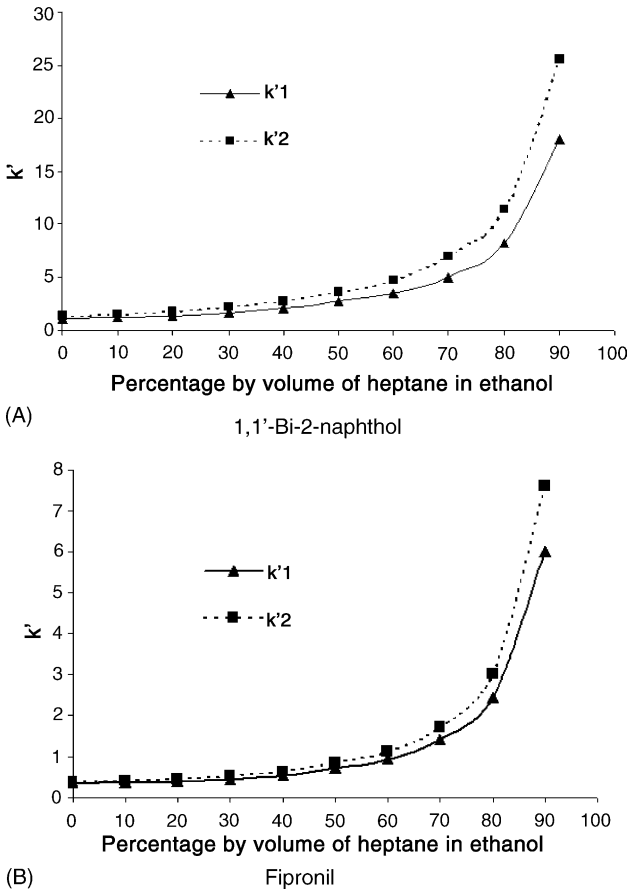

Fig. 2. Normal-phase retention behavior of the first and second eluted enantiomers of (A) 1,1′-bi-2-naphthol, and (B) fipronil as a function of mobile phase composition. The mobile phases consisted of various ratios of ethanol and heptane. The column was a 250 mm × 4.6 mm (i.d.) (*R*,*R*) P-CAP CSP (5 μm silica gel support). Flow rate: 1.0 ml/min at ambient temperature (~23 °C). Detection: UV at 254 nm.

Table 1
Chromatographic data for the traditional normal-phase resolution of racemic compounds on (*R*,*R*) P-CAP column

No.	Compounds	Structure	k'_1	k'_2	α	R_s	Mobile phase[a]
1	Hydrobenzoin	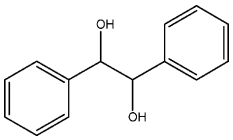	3.43	3.97	1.16	1.91	Heptane/IPA/TFA 80/20/0.1
2	Warfarin	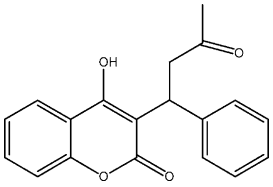	11.21	12.65	1.13	1.58	Heptane/IPA/TFA 90/10/0.1
3	1,1′-bi-2-Naphthol	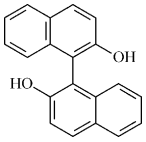	2.49	3.36	1.35	2.84	Heptane/EtOH/TFA 50/50/0.1
4	di-6,6′-Methoxy-bi-2-naphthol	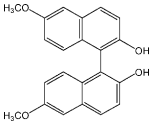	2.69	3.41	1.27	2.7	EtOH/Heptane 50/50
5	Dioxibrassinin	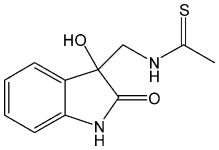	7.67	8.81	1.15	1.4	EtOH/Heptane 30/70 (v/v)
6	Indapamide	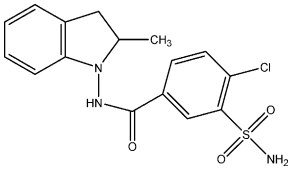	7.32	7.74	1.06	0.60	Heptane/EtOH/TFA 60/40/0.1
7	3-(α-Acetonyl-4-chlorobenzyl)-4-hydroxy coumarin	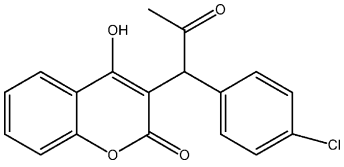	4.06	4.76	1.17	1.63	Heptane/IPA 80/20
8	*N*-3,5-dinitrobenzoyl-DL-leucine	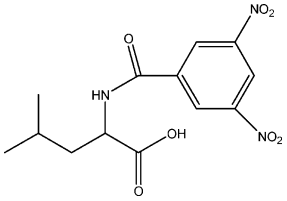	7.65	8.32	1.09	0.79	Heptane/EtOH/TFA 90/10/0.1 2 ml/min
9	Bendroflumethiazide	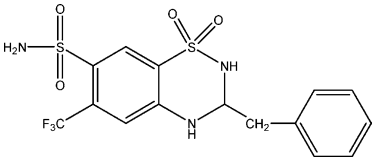	14.53	16.34	1.12	0.80	Heptane/IPA/TFA 50/50/0.1
10	*N*,*N*′-bis(α-Methyl benzyl)sulfamide	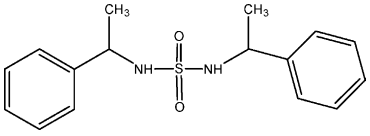	12.31	13.50	1.10	0.90	Heptane/IPA/TFA 80/20/0.1
11	2,3-*O*-Benzylidene-D-threitol	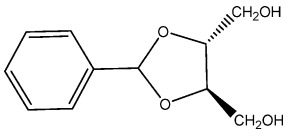	5.49	6.13	1.12	1.21	Heptane/IPA 80/20

Table 1 (*Continued*)

No.	Compounds	Structure	k'_1	k'_2	α	R_s	Mobile phase[a]
12	α-Carbethoxy-γ-phenyl-γ-butyrolactone	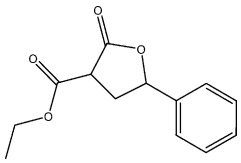	2.73	3.06	1.12	1.0	Heptane/IPA 80/20
13	Chlorthalidone	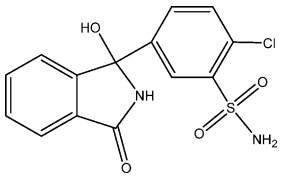	10.21	12.57	1.23	1.61	Heptane/EtOH/TFA 80/20/0.1
14	1,5-Dihydroxy-1,2,3,4-tetrahydro naphthalene	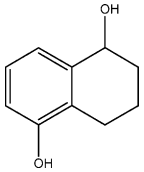	6.78	7.22	1.06	0.81	Heptane/IPA 80/20
15	DL-3,4-Dihydroxyphenyl-α-propylacetamide	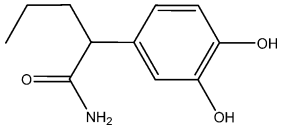	3.84	4.59	1.20	1.64	Heptane/EtOH/TFA 50/50/0.1
16	4-(Diphenylmethyl)-2-oxazolidinone	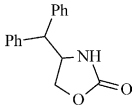	8.57	9.31	1.09	0.82	Heptane/IPA 80/20
17	1,1′-bi-(2-naphthylamine)	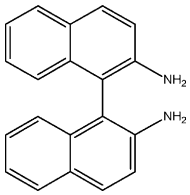	5.80	5.95	1.03	0.7	Heptane/IPA 80/20
18	cis-4,5-Diphenyl-2-oxazolidinone	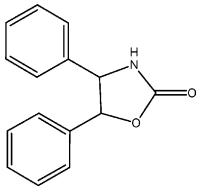	12.64	13.72	1.09	1.22	Heptane/IPA/TFA 90/10/0.1
19	5-Ethyl-5,6-dihydro-3,8-dinitro-6-phenyl-6-phenanthridinol	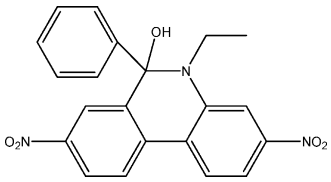	5.43	5.75	1.06	1.05	Heptane/EtOH/TFA 80/20/0.1
20	5-Fluoro-1-(tetrahydro-2-furfuryl)uracil	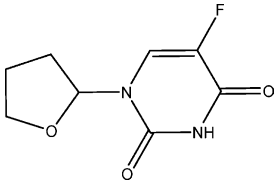	5.04	5.39	1.07	0.65	Heptane/EtOH/TFA 90/10/0.1 2 ml/min
21	DL-3-(4-Hydroxyphenyl)lactic acid	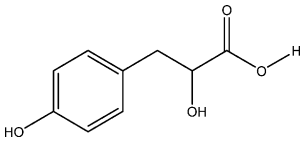	4.57	5.76	1.26	1.54	Heptane/IPA/TFA 60/40/0.1

Table 1 (*Continued*)

No.	Compounds	Structure	k'_1	k'_2	α	R_s	Mobile phase[a]
22	Mandelamide	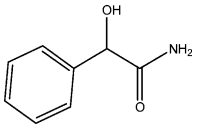	9.62	11.53	1.20	1.50	Heptane/IPA/TFA 80/20/0.1
23	5-Methyl-5-phenyl hydantoin	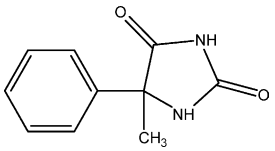	8.33	9.06	1.09	0.9	Heptane/IPA 80/20
24	cis-4-Methyl-5-phenyl-2-oxazolidinone	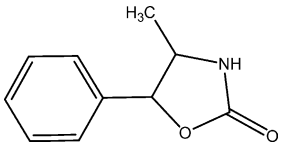	10.32	11.37	1.10	1.52	Heptane/IPA/TFA 80/20/0.1
25	*N*-(α-Methylbenzyl)-phthalamic acid	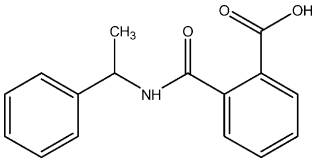	3.98	4.19	1.05	0.72	Heptane/EtOH/TFA 80/20/0.1
26	Methyl mandelate	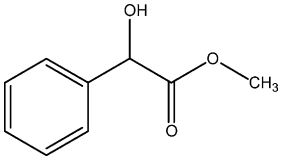	1.93	2.47	1.13	1.2	Heptane/IPA 80/20
27	Benzyl mandelate	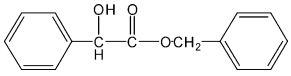	2.07	2.21	1.07	1.0	EtOH/Heptane 10/90
28	Mandelic acid	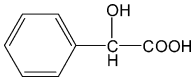	2.04	2.19	1.07	1.0	EtOH/Heptane 10/90
29	DL-3-Phenyllactic acid	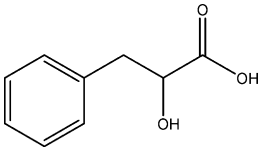	1.64	2.01	1.23	1.28	Heptane/EtOH/TFA 60/40/0.1
30	1-Phenyl-1,2-ethane diol	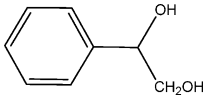	4.68	5.25	1.12	1.60	Heptane/IPA 80/20
31	γ-Phenyl-γ-butyrolactone	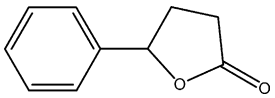	2.82	3.00	1.06	0.92	Heptane/IPA 80/20
32	Phenylsuccinic anhydride	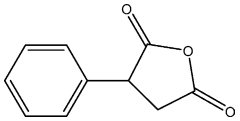	2.68	3.05	1.14	1.45	Heptane/EtOH/TFA 70/30/0.1
33	(3a(*R*,*S*)-cis)-3,3a,8,8a-Tetrahydro-2H-indeno[1,2-d]oxazol-2-one	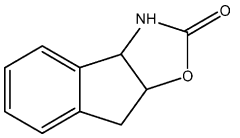	7.77	9.36	1.20	1.66	Heptane/IPA/TFA 80/20/0.1
34	Fipronil	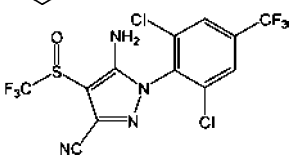	4.11	6.13	1.49	3.73	Heptane/IPA/TFA 20/80/0.1
35	*trans*-1,2-cyclohexanediyl-bisacrylamide (DACH-ACR)	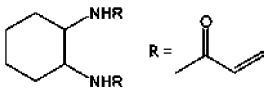	0.78	1.02	1.31	2.7	EtOH/Heptane 10/90

Table 1 (*Continued*)

No.	Compounds	Structure	k'_1	k'_2	α	R_s	Mobile phase[a]
36	*trans*-1-(2-Amino-cyclohexyl)-3-(3,5-bis-trifluoromethyl-phenyl)-urea	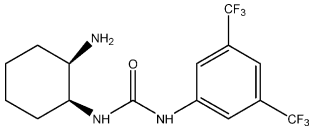	1.97	2.11	1.07	0.65	EtOH/Heptane/TFA 10/90/0.1
37	*trans*-(1,2)-Diaminocyclohexyl di(4-vinyl) benzoylamide	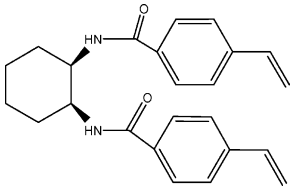	0.30	0.50	1.68	1.25	EtOH/Heptane 50/50
38	Lorazepam	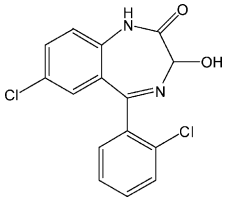	3.48	5.26	1.51	4.2	EtOH/Heptane 50/50 (v/v)
39	Oxazepam	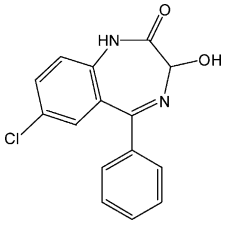	3.31	5.03	1.52	4.3	EtOH/Heptane 50/50
40	4-Chlorophenyl methyl sulfoxide	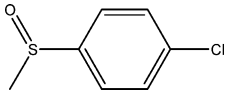	3.81	4.09	1.07	0.78	Heptane/IPA/TFA 90/10/0.1
41	Methyl 4-trifluoromethylphenyl sulfoxide	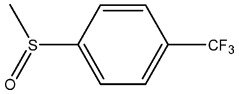	3.30	3.58	1.08	0.92	Heptane/IPA/TFA 90/10/0.1
42	4-Fluorophenyl methyl sulfoxide	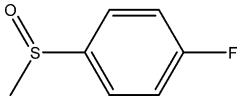	4.31	4.54	1.05	0.65	Heptane/IPA/TFA 90/10/0.1
43	4-Bromophenyl methyl sulfoxide	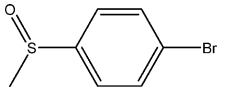	3.83	4.13	1.08	0.88	Heptane/IPA/TFA 90/10/0.1

(*R*,*R*) P-CAP was bonded to 5 μm silica gel and the stationary phase was packed in a 250 mm × 4.6 mm (i.d.) stainless steel column.

[a] All samples were analyzed under the chromatographic condition: a UV detector at 254 nm, flow rate 1 ml/min, unless otherwise noted. All mobile phase ratios were volume to volume. IPA: 2-propanol. TFA: trifluoroacetic acid.

1,1′-bi-2-naphthol as a function of polar organic mode mobile phase composition. The resolution (R_s) curve has a minimum at a mobile phase composition of acetonitrile/methanol 30/70 (v/v). The maximum of retention factor k'_1 of the first eluted enantiomer, selectivity factor α, and resolution R_s are all at 100% acetonitrile.

3.2.2. Effects of mobile phase additives

Additives to the mobile phase can usually improve chromatographic efficiency. Trifluoroacetic acid (TFA) is the most effective additive in both the normal-phase mode and the polar organic mode. Ammonium acetate sometimes can also be used in the polar organic mode as an additive. These additives usually shorten the retention time, decrease tailing and sharpen the peaks. Fig. 4 shows the enantiomeric separation of (*R*,*R*)- and (*S*,*S*)-hydrobenzoin on the (*R*,*R*) P-CAP column with different composition of normal-phase solvents. The best separation (Chromatogram A) was achieved when heptane/2-propanol/TFA 80/20/0.1 was used as the mobile phase. Without the TFA additive (Chromatogram B), only a partial separation can be achieved and the peaks become broader.

Three probe molecules, including chlorthalidone, sulindac, and (±)-2,3-dibenzoyl-DL-tartaric acid, were chosen to investigate the influence of acid additives in polar organic mode. The results are summarized in Table 4. Chlorthalidone ($pK_a = 9.4$) is a weak base. The acid additives, acetic acid and TFA, have almost no influence on separation

Table 2
Chromatographic data for the polar organic mode resolution of racemic compounds on (*S*,*S*) P-CAP column or (*R*,*R*) P-CAP column

No	Compounds	Structure	k'_1	k'_2	α	R_s	Mobile phase[a]
1	4-Methoxy-2-phenyl-4,5,6,7-tetrahydro-benzofuran-3-carboxylic acid	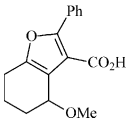	1.0	1.17	1.17	1.22	CH_3CN/CH_3OH/TFA 99/1/0.1
2	Sulindac	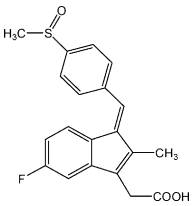	4.03	4.62	1.15	1.85	CH_3CN/CH_3OH/TFA 99/1/0.1
3	Benzoin	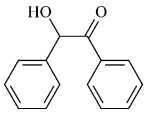	0.43	0.56	1.30	1.18	$CH_3CN/CH_3OH/NH_4OAc$ 99/1/10 mM (v/v/C)
4	DL-β-Phenyllactic acid	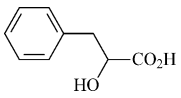	3.99	4.34	1.09	0.93	CH_3CN/CH_3OH/TFA 95/5/0.1
5	(±)-1,1′-bi-2-Naphthol	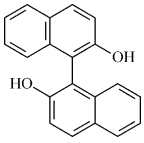	1.47	1.97	1.34	3.80	ACN/MeOH/NH_4OAc[b] 95/5/10 mM (v/v/C)
			1.86	2.54	1.36	3.43	CH_3CN/CH_3OH/TFA[b] 95/5/0.1
6	Althiazide	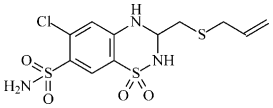	4.79	5.28	1.10	0.50	$CH_3CN/CH_3OH/NH_4OAc$ 95/5/10 mM (v/v/C)
7	Benzoin methyl ether	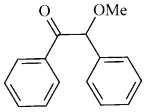	0.43	0.61	1.42	1.03	CH_3CN
8	(±)*N*,*N*-bis-(α-Methylbenzyl) sulfamide	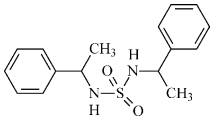	0.70	0.93	1.33	1.02	CH_3CN
9	Bendroflumethiazide	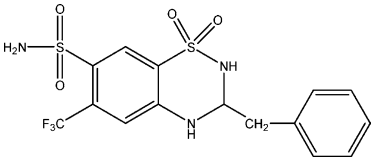	4.39	4.86	1.11	0.51	$CH_3CN/CH_3OH/NH_4OAc$ 95/5/10 mM (v/v/C)
10	3-(4-Chlorophenyl)-2-ethyl-2,3,5,6-tetrahydroimidazol [2,1-b]-thiazol-3-ol	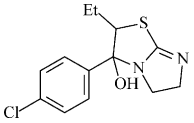	2.34	2.59	1.11	0.94	CH_3CN/HOAc/TEAA 100/0.25/0.05
11	Chlorthalidone	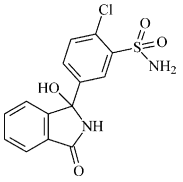	5.02	6.92	1.38	2.5	CH_3CN/CH_3OH/TFA 90/10/0.1

Table 2 (*Continued*)

No	Compounds	Structure	k'_1	k'_2	α	R_s	Mobile phase[a]
12	*p*-Chloromandelic acid	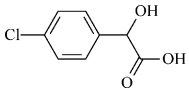	7.06	8.08	1.14	1.65	CH_3CN/CH_3OH/TFA 99/1/0.1
13	7-(2,3-Dihydroxypropyl) theophylline	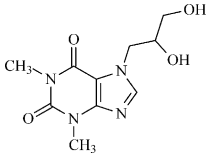	2.23	2.44	1.09	0.72	CH_3CN/HOAc/TEAA 100/0.25/0.05
14	(±)-4-(Diphenylmethyl)-2-oxazolidinone	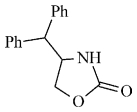	0.61	0.74	1.21	1.06	$CH_3CN/CH_3OH/NH_4OAc$ 99/1/10 mM (v/v/C)
15	(±)-2,3-Dibenzoyl-DL-tartaric acid	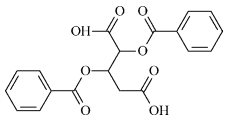	9.26	10.15	1.10	0.94	CH_3CN/CH_3OH/TFA 95/5/0.1
16	DL-*p*-Hydroxymandelic acid	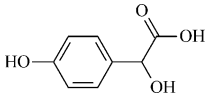	9.40	10.43	1.11	0.95	CH_3CN/CH_3OH/TFA 95/5/0.1
17	DL-3-(4-hydroxyphenyl)lactic acid hydrate	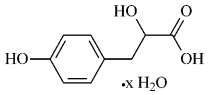	3.24	3.56	1.10	1.05	CH_3CN/CH_3OH/TFA 90/10/0.1
18	3-[2-Methylphenoxy]-1,2-propanediol	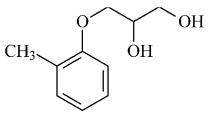	1.48	1.56	1.05	0.50	CH_3CN/HOAc/TEAA 100/0.25/0.05
19	DL-Mandelic acid	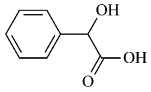	5.30	5.90	1.11	1.29	CH_3CN/CH_3OH/TFA 99/1/0.1
20	DL-Mandelamide	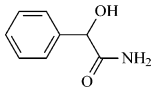	1.96	2.24	1.14	1.00	CH_3CN/CH_3OH/TFA 99/1/0.1
21	(±)-*N*-(α-Methylbenzyl) phthalic acid monoamide	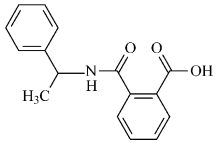	2.80	3.22	1.15	0.88	CH_3CN/CH_3OH/TFA 99/1/0.1
22	(±)-Phenylsuccinic anhydride	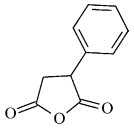	2.42	2.90	1.20	2.62	CH_3CN/CH_3OH/TFA 90/10/0.1
23	3a,4,5,6-Tetrahydro-succinimido[3,4-b] acenaphthen-10-one	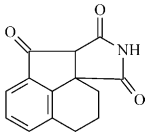	1.28	1.47	1.15	0.37	CH_3CN/HOAc/TEAA 100/0.25/0.05
24	DL-Tropic acid	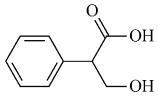	4.87	5.71	1.17	1.90	CH_3CN/CH_3OH/TFA 99/1/0.1
25	(3a[*R*,*S*]cis)-(±)-3,3a,8,8a-Tetrahydro-2H-indeno[1,2-d]-oxazol-2-one	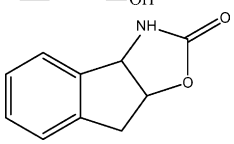	0.64	0.79	1.22	1.03	CH_3CN/HOAc/TEAA 100/0.25/0.05
26	(±)-1-Phenyl-1,2-ethanediol	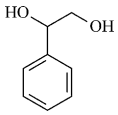	1.35	1.45	1.07	0.56	CH_3CN/HOAc/TEAA 100/0.25/0.05

Table 2 (*Continued*)

No	Compounds	Structure	k'_1	k'_2	α	R_s	Mobile phase[a]
27	(±)-2,2,2-Trifluoro-1-(9-anthryl) ethanol	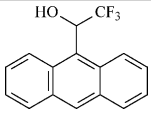	0.58	0.62	1.07	0.35	CH_3CN/HOAc/TEAA 100/0.25/0.05
28	1,1′-Binaphthyl-2,2′-diyl-H phosphate	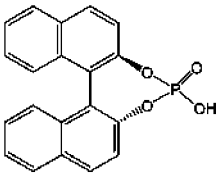	2.00	2.35	1.17	1.4	ACN/MeOH/NH_4OAc[b] 70/30/20 mM (v/v/C)
29	Diacetyl cysteine	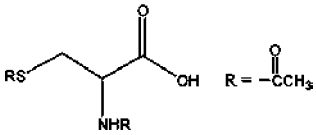	2.61	3.39	1.30	1.5	ACN/MeOH/NH_4OAc[b] 80/20/0.1 (v/v/w)
30	FMOC-phenylalanine	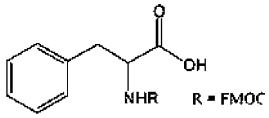	1.85	2.54	1.37	3.5	ACN/MeOH/TFA[b] 95/5/0.1 (v/v/v)
			1.17	1.43	1.22	2.1	ACN/MeOH/NH_4OAc[b] 70/30/20 mM (v/v/C)
31	2-Hydroxy-3-(Boc-amino)-3-phenylpropionic acid	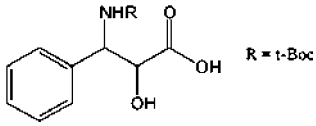	2.52	3.63	1.44	2.4	ACN/MeOH/TFA[b] 95/5/0.1 (v/v/v)
32	Lorazepam	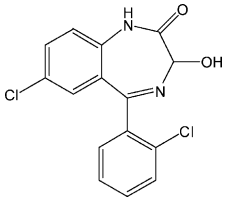	0.86	1.53	1.80	5.8	ACN/MeOH/NH_4OAc[b] 70/30/20 mM (v/v/C)
33	Oxazepam	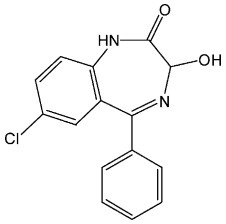	0.85	1.42	1.66	5.4	ACN/MeOH/NH_4OAc[b] 70/30/20 mM (v/v/C)
34	Diaminocyclohexane acrylamide (DACH-ACR)	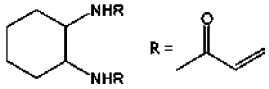	0.30	0.70	2.34	4.0	ACN/MeOH[b] 70/30

(*S*,*S*) P-CAP and (*R*,*R*) P-CAP were bonded to 5 μm silica gel and the stationary phase was packed in a 250 mm × 4.6 mm (i.d.) stainless steel column. All data shown were run on (*S*,*S*) P-CAP column unless otherwise noted.

[a] All samples were analyzed under the chromatographic condition: a UV detector at 254 nm, flow rate l ml/min, unless otherwise noted. All mobile phase ratios were volume to volume. TEAA: triethylammonium acetate. TFA: trifluoroacetic acid. ACN: acetonitrile.

[b] On (*R*,*R*) P-CAP column.

factor α, and a minor influence on the resolution (R_s). Under the same solvent system with the same volume ratio of acid additives, TFA increases the R_s more than acetic acid does. Sulindac ($pK_a = 4.7$) has one carboxylic acid group. It could not be eluted with a mobile phase of $CH_3CN/CH_3OH = 95/5$, without acid additives. The compound (±)-2,3-dibenzoyl-DL-tartaric acid has two carboxylic acid groups. It is the strongest acid among three analytes. With the mobile phase of $CH_3CN/CH_3OH = 95/5$, it can only be eluted with the addition of 0.1% trifluoroacetic acid. The acid additives protonate acidic analytes as well as any residual amine groups on the stationary phase (e.g. from the 3-aminopropylsilanized silica gel). This minimizes a source of strong non-enantioselective association between acidic analytes and the CSP. The additives therefore improve the mass transfer and thus improve the efficiency. Compared

Table 3
Chromatographic data for the normal-phase mode with halogenated solvent and other mobile phases resolution of racemic compounds on (*R*,*R*) P-CAP column

No.	Compounds	Structure	k'_1	k'_2	α	R_s	Mobile phase[a]
1	1,1′-bi-2-Naphthol	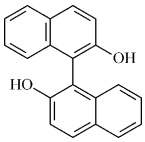	0.95	1.65	1.74	3.40	Acetone
			1.47	2.39	1.63	3.85	CH_2Cl_2/MeOH 95/5
2	Hydrobenzoin	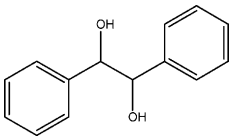	2.94	3.41	1.16	1.48	CH_2Cl_2/MeOH 99/1
3	Indapamide	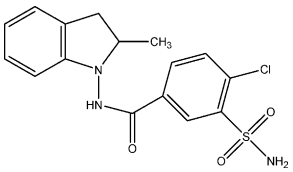	4.19	4.33	1.03	0.49	CH_2Cl_2/MeOH 95/5
4	3-(α-Acetonyl-4-chlorobenzyl)-4-hydroxy coumarin	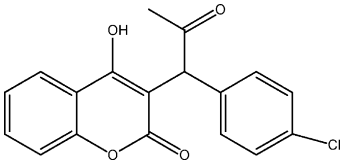	0.77	0.83	1.08	0.68	CH_2Cl_2/MeOH 95/5
5	1,5-Dihydroxy-1,2,3,4-tetrahydro-naphthalene	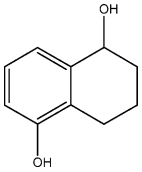	7.03	8.17	1.16	1.84	CH_2Cl_2/MeOH/TFA 98/2/0.1
8							
6	Mephenesin	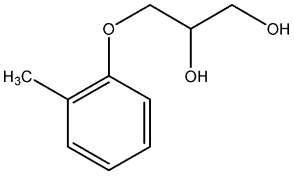	3.85	4.15	1.08	0.67	CH_2Cl_2/MeOH/TFA 98/2/0.1
7	Mandelamide	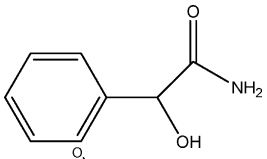	3.60	4.15	1.15	1.93	CH_2Cl_2/MeOH 95/5
8	5-Methyl-5-phenylhydantoin	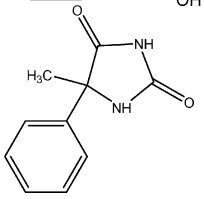	5.70	5.91	1.04	0.74	CH_2Cl_2/MeOH 95/5
9	3a,4,5,6-Tetrahydrosuccinimido[3,4-b] acenaphthen-10-one	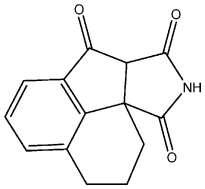	5.00	5.27	1.06	0.46	CH_2Cl_2/MeOH 99/1
10	(3a[*R*,*S*]-cis)-3,3a,8,8a-Tetrahydro-2H-indeno[1,2-d]oxazol-2-one	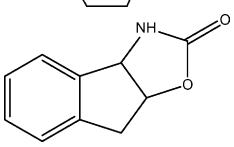	4.18	4.73	1.13	1.45	CH_2Cl_2/MeOH 99/1 (v/v)

(*R*,*R*) P-CAP was bonded to 5 μm silica gel and the stationary phase was packed in a 250 mm × 4.6 mm (i.d.) stainless steel column.

[a] All samples were analyzed under the chromatographic condition: a UV detector at 254 nm, flow rate 1 ml/min, unless otherwise noted. All mobile phase ratios were volume to volume. TEAA: triethylammonium acetate.

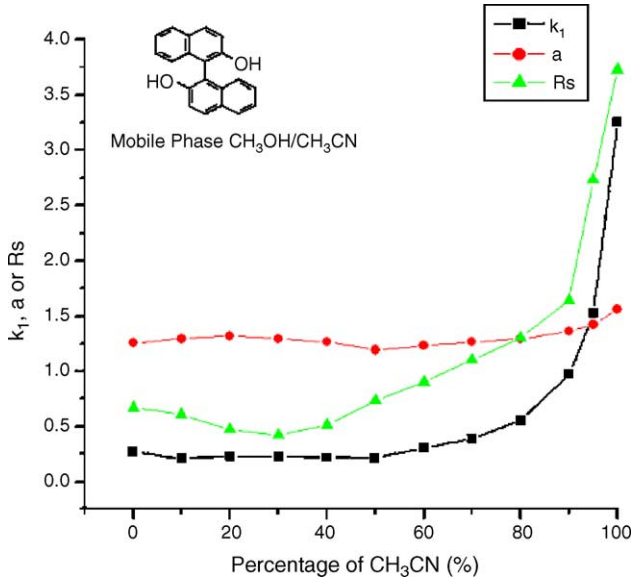

Fig. 3. Polar organic phase retention factor k'_1 of the first eluted enantiomer, selectivity factor a, and resolution R_s of 1,1′-bi-2-naphthol as a function of mobile phase composition. The mobile phases consisted of various ratios of methanol and acetonitrile. The column was a 250 mm × 4.6 mm (i.d.) (*S*,*S*) P-CAP CSP (5 μm silica gel support). Flow rate: 1.0 ml/min at ambient temperature (~23 °C). Detection: UV at 254 nm.

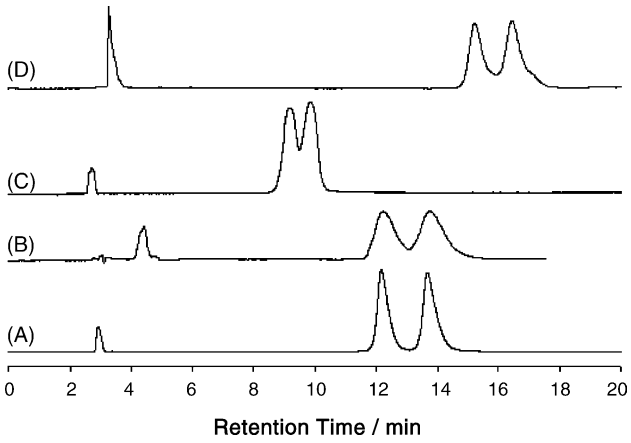

Fig. 4. Resolution of (*R*,*R*)- and (*S*,*S*)-hydrobenzoin on (*R*,*R*) P-CAP in the normal phase: (A) heptane/2-propanol/trifluoroacetic acid 80/20/0.1 (v/v/v); (B) heptane/2-propanol 80/20 (v/v); (C) heptane/EtOH/trifluoroacetic acid 80/20/0.1 (v/v/v). (D) heptane/EtOH/trifluoroacetic acid 90/10/0.1 (v/v/v). Flow rate: 1.0 ml/min; UV detection at 254 nm, T = 23 °C.

to acetic acid, TFA is a stronger acid and produces better separations.

3.2.3. *Normal-phase modifier*

The choice of organic modifier in the normal-phase mode (i.e. ethanol, 2-propanol, etc. in *n*-heptane) affects the efficiency, retention, and the resolution of enantiomers. In Fig. 4, 2-propanol is used as normal-phase modifier for Chromatogram A. While for Chromatogram C, ethanol is used instead of 2-propanol. A baseline separation was achieved within 15 min with the mobile phase of heptane/2-propanol/TFA 80/20/0.1. But for ethanol, with the same mobile phase ratio (heptane/ethanol/TFA 80/20/0.1), only a partial separation (R_s 0.8) was achieved. When decreasing the ratio of ethanol to 10% (Chromatogram D in Fig. 4, mobile phase: Heptane/ethanol/TFA 90/10/0.1), the retention time is comparable to that of Chromatogram A, but the separation still was not baseline even with a longer retention time. In both cases, a TFA additive was used. Separations of some other compounds in the normal-phase mode, such as

Table 4
Effect of acid additives on selectivity and resolution for the polar organic mode enantiomeric separations on (*S*,*S*) P-CAP column

Name	Structure	k'_1	α	R_s	Mobile phase
Chlorthalidone	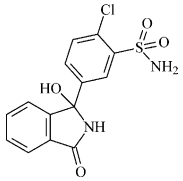	5.00	1.38	2.0	CH_3CN/CH_3OH = 90/10
		5.11	1.37	2.1	CH_3CN/CH_3OH/HOAc = 90/10/0.1
		5.02	1.38	2.5	CH_3CN/CH_3OH/TFA = 90/10/0.1
Sulindac	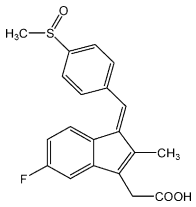	No elution			CH_3CN/CH_3OH = 95/5
		2.33	1.11	1.0	CH_3CN/CH_3OH/HOAc = 95/5/0.1
		2.16	1.12	1.0	CH_3CN/CH_3OH/TFA = 95/5/0.1
(±)-2,3-Dibenzoyl-DL-tartaric acid	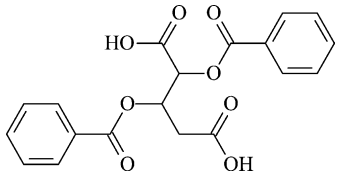	No elution			CH_3CN/CH_3OH = 95/5
		No elution			CH_3CN/CH_3OH/HOAc = 95/5/0.1
		9.26	1.10	0.94	CH_3CN/CH_3OH/TFA = 95/5/0.1

The sample was analyzed with a UV detector at 254 nm. Flow rate: 1 ml/min. Ambient temperature (~23 °C).

Table 5
Effect of flow rate on selectivity and resolution for the normal-phase enantiomeric separations of fipronil on (*R*,*R*) P-CAP column

Compound	Flow rate (ml/min)	k'_1	k'_2	Selectivity (α)	Resolution (R_s)
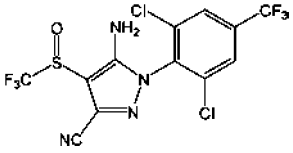	0.5	2.35	2.87	1.22	1.71
	1.0	2.30	2.80	1.22	1.57
	1.5	2.27	2.76	1.22	1.46
	2.0	2.24	2.73	1.22	1.40

The mobile used to enantioseparate fipronil consisted of heptane/ethanol/TFA 80/20/0.1. The sample was analyzed with a UV detector at 254 nm.

Table 6
Efficiency comparison of enantioseparation of 1.1′-bi-2-naphthol in the traditional normal-phase mode, polar organic mode and the normal-phase mode with halogenated solvent system on (*R*,*R*) P-CAP column

Mobile phase	Enantioselectivity (α)	Enantioresolution (R_s)	Number of theoretical plates[a] (N)
The traditional normal-phase mode (heptane/EtOH/TFA 30/70/0.1)	1.32	1.86	1704
Polar organic mode (acetonitrile/MeOH/TFA 95/5/0.1)	1.36	3.43	3552
The normal-phase with halogenated solvent system (methylene chloride/MeOH 95/5).	1.54	4.03	6042

The sample was analyzed at the flow rate of 1 ml/min, with a UV detector at 254 nm under room temperature (~23 °C).
[a] Theoretical plates (N) are based on the second eluted enantiomer.

fipronil, produced the same general trend. For these chiral stationary phases, 2-propanol was a better normal mobile phase modifier than ethanol.

3.2.4. Effect of mobile phase flow rate

The effect of mobile phase flow rate on enantiomeric selectivity and resolution in the normal-phase mode also was evaluated. Table 5 shows the chromatographic data of the normal-phase enantiomeric separations of fipronil on the (*R*,*R*) P-CAP column at flow rates of 0.5, 1.0, 1.5 and 2.0 ml/min. As can be seen, flow rate has little or no effect on enantioselectivity, while resolution is affected. The resolution is improved from 1.40 to 1.71 if the flow rate is decreased from 2.0 to 0.5 ml/min. This is because of the mass transfer in the stationary phase affects efficiency at higher flow rates [33]. This is a common phenomenon for other CSPs. For high throughput screening, one can use higher flow rates, like 2.0 ml/min, and still gets reasonable resolution.

3.2.5. Column efficiency in different mobile phase modes

The normal-phase mode with two different solvent systems (heptane/IPA and methylene chloride/methanol) and the polar organic mode can be used on P-CAP columns. Table 6 shows the chromatographic data for the enantiomeric separation of 1,1′-bi-2-naphthol in different mobile phases. As can be seen in Table 6, the halogenated mobile phase gives the highest efficiency (greatest N). The polar organic mode produces intermediate efficiency and the traditional normal-phase separations are the least efficient among three mobile phase systems. However, as noted previously (see Tables 1 and 2), far more compounds are separated with a heptane/IPA mobile phase than with a methylene chloride-based mobile phase.

3.2.6. Sample loading capacity

P-CAP columns are polymeric CSPs. The high loading of the chiral selector on the silica gel provides the potential of having a high sample loading capacity. Fig. 5 shows the chromatogram of the separation of 1,1′-bi-2-naphthol when 1 and 1000 μg racemic sample was injected sequentially. As can be seen, the resolution is still nearly 1.5 even with a thousand times greater sample load on an analytical column. Clearly,

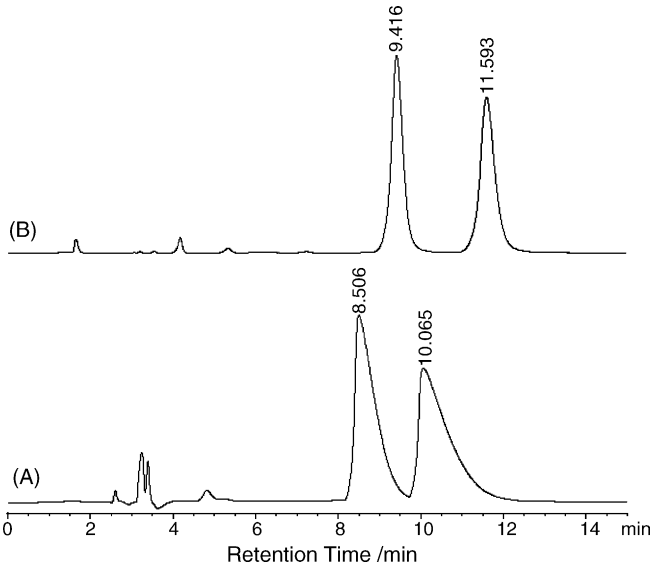

Fig. 5. Sample loading capacity test for the separation of 1,1′-bi-2-naphthol on (*R*,*R*) P-CAP column. Sample loading (A) 1000 μg; (B) 1 μg. (*R*,*R*) P-CAP was bonded to 5 μm silica gel and the stationary phase was packed in a 250 mm × 4.6 mm (i.d.) stainless steel column. Mobile phase: EtOH/heptane 50/50; flow rate: l ml/min; detection: UV at 254 nm; temperature: ~23 °C. This figure is reproduced with permission of Astec, Whippany, NJ, USA. (http://www.astecusa.com/).

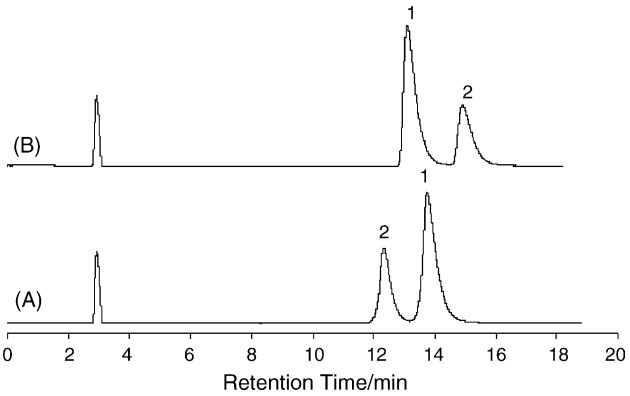

Fig. 6. Reversal of elution order on (A) (*R*,*R*) P-CAP and (B) (*S*,*S*) P-CAP columns under the normal phase. Peak 1 is (*R*,*R*)-hydrobenzoin and Peak 2 is (*S*,*S*)-hydrobenzoin with the mole ratio of (*R*,*R*):(*S*,*S*) = 2:1. Mobile phase: heptane/2-propanol/TFA 80/20/0.1 (v/v/v); flow rate: l ml/min; UV detection at 254 nm; $T = 23\,^{\circ}C$.

the P-CAP CSPs are suitable for large-scale enantiomeric separations.

3.3. Reversal of elution order

The totally synthetic chiral selectors of the (*R*,*R*) P-CAP column and the (*S*,*S*) P-CAP column have the opposite absolute configuration. Therefore, the elution order of all separable enantiomers will be inverted on these two columns. Fig. 6 shows the inversion of elution order on (*R*,*R*) P-CAP column and the (*S*,*S*) P-CAP column under normal phase conditions. The (*R*,*R*)- and (*S*,*S*)-hydrobenzoin were chosen as example probe molecules. In order to identify the enantiomeric peaks of the probe molecules easily, the analyte sample containing (*R*,*R*)- and (*S*,*S*)-hydrobenzoin was prepared in the mole ratio of 2 to 1, respectively. Fig. 6 also shows that (*R*,*R*) P-CAP CSP retains (*R*,*R*)-hydrobenzoin longer than its (*S*,*S*)-enantiomer, and of course, the (*S*,*S*) P-CAP CSP retains (*S*,*S*)-hydrobenzoin to a greater extent.

Interestingly, the (*R*,*R*)- and (*S*,*S*) P-CAP columns can also separate their mixed monomers DACH-ACR very well. Fig. 7 shows the chromatographic separation of DACH-ACR on both (*R*,*R*)- and (*S*,*S*) P-CAP column. As can be seen from Fig. 8, the (*R*,*R*) P-CAP column retains (*S*,*S*)-DACH-ACR more and the (*S*,*S*) P-CAP column favors (*R*,*R*)-DACH-ACR.

3.4. Interactions for chiral recognition

The P-CAP columns do not contain any aromatic moieties. Therefore, π–π interactions are not important with this CSP. Instead, the P-CAP CSPs have large numbers of amide linkages, which provide hydrogen bonding and dipolar interactions between these CSPs and chiral analytes. An examination of the compounds listed in Tables 1–3 reveals a common

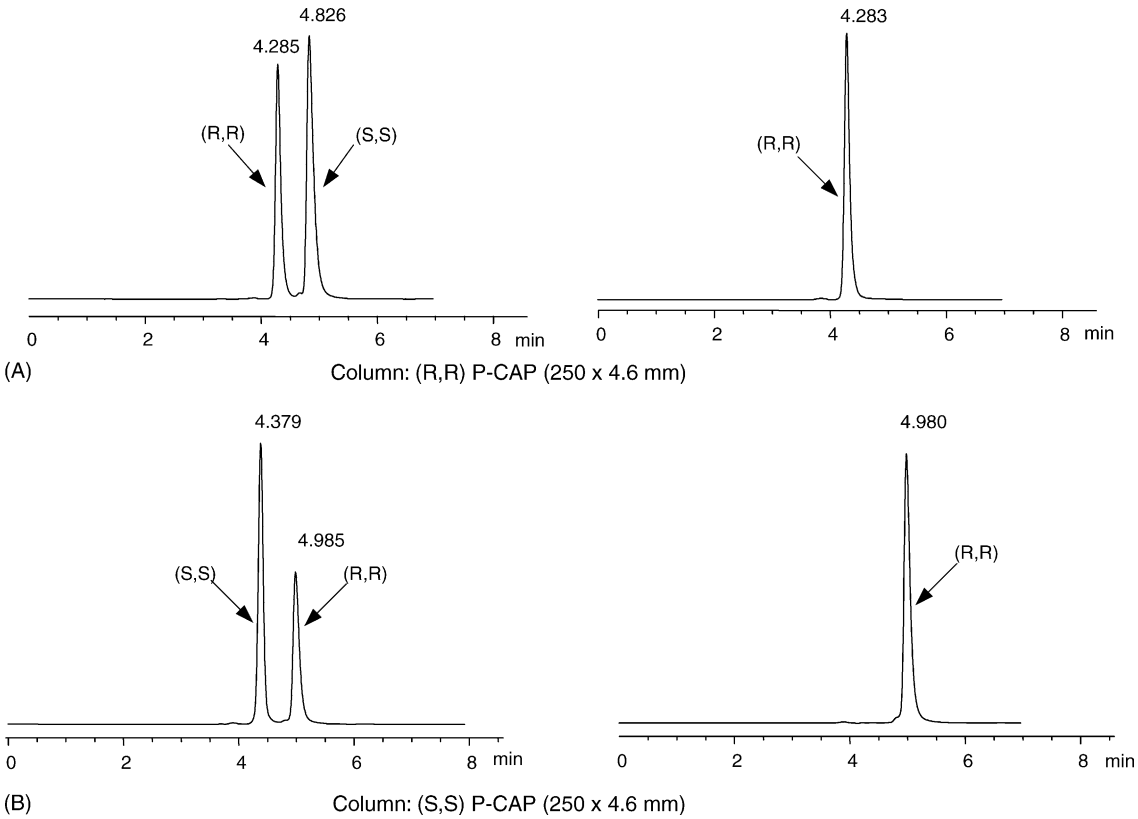

Fig. 7. Reverse elution order on (A) (*R*,*R*) P-CAP and (B) (*S*,*S*) P-CAP CSPs under polar organic phase. Analytes were the mixture of (*R*,*R*) DACH-ACR and (*S*,*S*) DACH-ACR. Mobile Phase: 85/15/10 mM ACN/MeOH/NH_4OAc. Flow rate: 0.8 ml/min. Detection: UV at 254 nm. Temperature: 25 °C. (A) Column: (*R*,*R*) P-CAP (250 mm × 4.6 mm); (B) column: (*S*,*S*) P-CAP (250 mm × 4.6 mm).

characteristic for these compounds. Most of them contain a hydroxyl group, carboxylic group, carbonyl, amine, amide, urea, or fluorine group, all of which are capable of forming strong hydrogen bonds. Thus, hydrogen bond interactions are believed to be the dominant associative interactions for chiral recognition by P-CAP CSPs [19].

Some chiral sulfoxides also were resolved on P-CAP columns. These sulfoxides include 4-chlorophenyl methyl sulfoxide and 4-bromophenyl methyl sulfoxide, etc. These chiral sulfoxides are known to possess a strong dipolar element and the amide linkage in the P-CAP CSPs also is strongly dipolar. Therefore, dipole-dipole interaction also may be important for chiral discrimination on the P-CAP CSPs.

The cyclohexyl moiety (Fig. 1) is a restricted configurational nonpolar unit of the P-CAP stationary phase. It may provide solvophobic-driven attraction or steric repulsive effects. These are possible interactions for enantiomeric selectivity by these CSPs.

4. Conclusions

The polymeric (*R*,*R*) and (*S*,*S*) poly (*trans*-1,2-cyclohexanediyl-bis acrylamide) (known as (*R*,*R*) P-CAP and (*S*,*S*) P-CAP) have been used as liquid chromatographic chiral stationary phases. The branched polymer was bonded covalently to a 5 μm silica gel support and evaluated for enantiomeric separations. P-CAP CSPs can be used in the normal-phase mode or the polar organic mode to produce enantiomeric separations of a variety of chiral compounds. The retention behavior, selectivity, and resolution were examined for selected compounds in each mobile phase mode. A total of 62 chiral compounds were enantioresolved on these two columns. The traditional normal phase separation mode was the most broadly selective, but has the lowest efficiency. Halogenated mobile phases produced the highest efficiencies but separated the fewest compounds. The polar organic mode was intermediate in terms of both selectivity and efficiency to the two normal phase approaches. The elution order of enantiomers can be reversed between (*R*,*R*)- and (*S*,*S*) P-CAP CSPs. P-CAP columns have great sample loading capacity and are therefore able to do large-scale separations. The P-CAP CSPs were chemically stable under the usual separation conditions and not irreversibly damaged or modified when changing the mobile phase modes.

Acknowledgements

Support of this work by the National Institutes of Health, NIH RO1 GM53825-08, and the Iowa Energy Center is gratefully acknowledged.

References

[1] D.W. Armstrong, Anal. Chem. 59 (1987) A84, A90.
[2] D.W. Armstrong, J. Liq. Chromatogr. 7 (1984) 353.
[3] E. Gil-Av, J. Mol. Evol. 6 (1975) 131.
[4] S.V. Rogozhin, V.A. Davankov, J. Chem. Soc. D-Chem. Commun. (1971) 490.
[5] D.W. Armstrong, LC–GC Curr. Issues HPLC Technol. (1997) S20.
[6] D.W. Armstrong, B. Zhang, Anal. Chem. 73 (2001) 557A.
[7] C. Yamamoto, Y. Okamoto, Bull. Chem. Soc. Jpn. 77 (2004), 227.
[8] C.A. White, G. Subramanian, in: G. Subramanian (Ed.), A Practical Approach to Chiral Separations by Liquid Chromatography, VCH, Weinheim, Germany, 1994 (Chapter 1).
[9] Y.L. Bennani, S. Hanessian, Chem. Rev. 97 (1997) 3161.
[10] J.F. Larrow, E.N. Jacobsen, Y. Gao, Y.P. Hong, X.Y. Me, C.M. Zepp, J. Organ. Chem. 59 (1994) 1939.
[11] T.A. Whitney, J. Organ. Chem. 45 (1980) 4214.
[12] R.I. Kureshy, N.H. Khan, S.H.R. Abdi, S.T. Patel, R.V. Jasra, Tetrahedron: Asymmetry 12 (2001) 433.
[13] A.M. Daly, C.T. Dalton, M.F. Renehan, D.G. Gilheany, Tetrahedron Lett. 40 (1999) 3617.
[14] C. Bied, J.J.E. Moreau, M.W.C. Man, Tetrahedron: Asymmetry 12 (2001) 329.
[15] R.I. Kureshy, N.U.H. Khan, S.H.R. Abdi, S.T. Patel, R.V. Jasra, Tetrahedron Lett. 42 (2001) 2915.
[16] Y.K. Kim, S.J. Lee, K.H. Ahn, J. Organ. Chem. 65 (2000) 7807.
[17] C. Altomare, S. Cellamare, A. Carotti, M.L. Barreca, A. Chimirri, A.M. Monforte, F. Gasparrini, C. Villani, M. Cirilli, F. Mazza, Chirality 8 (1996) 556.
[18] A. Brandi, S. Cicchi, F. Gasparrini, F. Maggio, C. Villani, M. Koprowski, K.M. Pietrusiewicz, Tetrahedron: Asymmetry 6 (1995) 2017.
[19] B. Galli, F. Gasparrini, D. Misiti, M. Pierini, C. Villani, M. Bronzetti, Chirality 4 (1992) 384.
[20] F. Gasparrini, D. Misiti, C. Villani, Chirality 4 (1992) 447.
[21] D. Kontrec, V. Vinkovic, A. Lesac, V. Sunjia, A. Aced, Enantiomer 5 (2000) 333.
[22] B. Gallinella, F. Latorre, R. Cirilli, C. Villani, J. Chromatogr. 639 (1993) 193.
[23] D.F. Johnson, J.S. Bradshaw, M. Eguchi, B.E. Rossiter, M.L. Lee, P. Petersson, K.E. Markides, J. Chromatogr. 594 (1992) 283.
[24] Y. Okamoto, Y. Nagamura, T. Fukumoto, K. Hatada, Polym. J. 23 (1991) 1197.
[25] Z. Juvancz, K.E. Markides, P. Petersson, D.F. Johnson, J.S. Bradshaw, M.L. Lee, J. Chromatogr. A 982 (2002) 119.
[26] K. Hu, J.S. Bradshaw, N.K. Dally, K.E. Krakowiak, N. Wu, M.L. Lee, J. Heterocyclic Chem. 36 (1999) 381.
[27] T. Nakano, J. Chromatogr. A 906 (2001) 205.
[28] Y. Okamoto, E. Yashima, M. Ishikura, K. Hatada, Bull. Chem. Soc. Jpn. 61 (1988) 255.
[29] Y. Okamoto, H. Mohri, M. Ishikura, K. Hatada, H. Yuki, J. Polym. Sci. Polym. Symp. (1986) 125.
[30] F. Gasparri, D. Misiti, C. Villani, WO 2003079002, 2003.
[31] F. Gasparrini, D. Misiti, C. Villani, Trac-Trends Anal. Chem. 12 (1993) 137.
[32] F. Gasparri, D. Misiti, C. Villani, R. Rompietti, Abstracts of the 15th International Symposium on Chirality (ISCD-15), Shizuoka, Japan, 2003, 132.
[33] D.W. Armstrong, Y.B. Liu, K.H. EkborgOtt, Chirality 7 (1995) 474.